Improving the Electrochemical Performances of Supercapacitors through Modification of the Particle Size Distribution of the Carbon Electrode

Improving the Electrochemical Performances of Supercapacitors through Modification of the Particle Size Distribution of the Carbon Electrode

Sutarsis[1,2*], Jeng-Kuei Chang[2,3]

[1] Department of Material and Metallurgy Engineering, Institut Teknologi Sepuluh Nopember, Kampus ITS Keputih, Surabaya, East Java, Indonesia 60111
[2] Graduate Institute of Material Science and Engineering, National Central University, 300 Zhongda Rd, Zhongli, Taoyuan 320, Republic of China
[3] Department of Material Science and Engineering, National Chiao Tung University, 1001 University Rd, East district, Hsinchu 300, Republic of China

*Email: sutarsis@mat-eng.its.ac.id

Abstract. The effect of a synergetic mixture of large and small activated carbon composite particles on the performance of organic electrolyte-based EDLCs was examined in this work. Different surface areas, pore volumes, particle size distributions, and concentrations of surface functional groups were observed in bi-modal particle sizes of activated carbon composites. Using galvanostatic cycling, the cell capacitance of an activated carbon composite rose with an increase in the fraction of big particles (C8) over a wide range of rates. Due to their moderate specific surface areas, a relatively low fraction of smaller particle size, low concentration of oxygen functional groups, low contact resistance, and high ionic conductivity, the 0.25C4+0.75C8 carbon electrode composite has a high specific capacitance, high retention of high rate discharge, and long cycle life when compared to other composites and single carbon electrodes (C4, C8, and C12). The leakage current and gas evolution may be suppressed to an operating voltage of 3.0 V with an appropriate fraction of large and small particle composition on the carbon electrode, boosting the carbon cells' reliability and stability.

1. Introduction

Because of its high power density, long cycle life, and several trustworthy safety features, supercapacitors, or SCs, are regarded to be an excellent complement to batteries for energy storage. As a result, SCs are commonly used to generate propulsive power in Electric Vehicles (EVs) and Hybrid Electrical Vehicles (HEVs) [1].

Because of their advantages, such as longer life, faster charging times, lighter and safer construction, no charging current limit, and maintenance-free operation, electrical double-layer capacitors (EDLCs) are the most common commercial SCs [2]. Power and energy densities in electrical double-layer capacitors (EDLCs) with porous carbon electrodes are known to be primarily reliant on the porosity, microstructure, and functional groups of the carbon particles, but particle size and distribution must also be considered [3, 4]. Although nanoscale materials like carbon nanotubes have been employed, their microstructure differs significantly from that of porous nanoparticles, with only the outer surface accessible for ion adsorption [5]. Another study looked at the impact of

activated carbon (ACs) particle size distribution on the performance of ionic liquid-based EDLCs. With a rising number of smaller ACs particles, capacitance, Columbic efficiency, and cycle life are all reduced. Furthermore, milling and sieving ACs to obtain sub-micrometer size fractions is a difficult and time-consuming procedure [6].

Different studies on the effect of particle size on the performance of EDLC electrodes, on the other hand, found that decreasing the average particle diameter improved capacitance and rate performance. The internal resistance of EDLCs increased as the average particle size (3.5−18.1 μm) increased, whereas the capacitance dropped, according to Yoshida et al. [7], This result was attributed to the denser packing of activated carbon at lower particle sizes, with the volume of voids increasing significantly with particle size. It was discovered that EDLCs with higher particle sizes had lower capacitance retention as the discharge rate increased [8]. By lowering the ion diffusion length, particle size reduction promotes ion transport. These studies concentrate on ideal particle size distributions, which are represented by a single parameter like average particle size. However, because the particle size distribution might comprise a wide range of particle sizes, comparing distinct populations of particles with a single particle size descriptor can be problematic.

Interparticle (or 'contact') resistances are the most important factor in the resistivity of powdered carbon in a packed bed. The shape of the particles and the compaction pressure applied to the bed determine interparticle resistance. The size, shape, and distribution of particle sizes affect bed packing and, as a result, the number of particle interactions, which can affect bed resistivity. When employing different particle size categories of the same carbon material, an increase in resistivity has been documented with decreasing particle size, which is due to a greater number of contacts per unit length [9]. In general, smaller particle sizes lead to more voids [10, 11]. The particle size distribution is likely to affect the resistance and performance of devices using composite electrodes due to the effect of particle size on total void volume and void sizes.

In this paper, we present an easier particle packing engineering method based on a mix of particle sizes between large and small ACs particles. Three ACs electrode composites (denoted as 0.75C4+0.25C8, 0.50C4+0.50C8, and 0.25C4+0.75C8) were evaluated and compared to the C4, C8 and C12 carbon electrodes. The influence of particle size distribution on the electrochemical performances and reliability were studied in organic electrolytes. In Polypropylene Carbonate (PC), composite electrodes was coupled with a 1 M tetraethylammonium tetrafluoroborate (TEA/BF_4) salt, and their performance in terms of specific capacitance, resistance, cycle life, leakage current, and gas evolution is evaluated to with concerning the fraction of each particle size of the activated carbon material.

2. Experimental methods

2.1 Materials

China Steel Co., Ltd supplied active material in the form of C4 (D_{50}=4.0 μm), C8 (D_{50}=8.2 μm), and C12 (D_{50}=11.9 μm) ACs. Aldrich Chemical Corp. provided electrolyte solutions such as TEA-BF_4 salt and Polypropylene Carbonate (PC). Other chemicals, such as a CMC and SBR binder, as well as carbon black and conductive carbon from a local supplier, were of analytical quality and utilized exactly as received. Cellulosic separator paper from Nippon Kodoshi Corporation Co. Ltd. is used in the EDLCs separator.

2.2 Active material design and electrode preparation

Small particles (C4) and big particles (C8) of ACs with the fractional composition of C4+xC8 (x=25 %, 50 %, and 75 %) were used to make carbon electrode composites. The investigation includes single carbon electrodes (C4, C8, and C12) as a comparison of their performance.

In deionized water, 91 wt% ACs powder, 2.5 wt% carbon black, 5 wt% styrenebutadiene rubber, and 1.5 wt% sodium carboxymethyl cellulose were mixed to make a carbon electrode slurry. The slurry was applied to etched Al-foil and vacuum dried for 6 hours at 90 °C. The coating layer's final thickness was 30 μm. After that, the electrode was perforated to fit the dimensions of a CR2032 coin

cell. In a coin cell, two symmetrical electrodes were separated by a cellulose separator. In PC, 1 M $TEABF_4$ salt (99 wt%, Alfa Aesar) was used as an electrolyte (99.7 wt%, Sigma-Aldrich). The coin cell construction was done in an argon-filled glovebox with a moisture and oxygen content of fewer than 0.3 parts per million.

2.3 Material characterizations and electrochemical measurements

The oxygen functional groups of the ACs samples were investigated using X-ray photoelectron spectroscopy (XPS; Thermo Fisher Scientific ESCALAB Xi^+). The X-ray source was chosen to be monochromatic AlK radiation. The binding energy calibration was done using the C1s peak of graphitic carbon, which is 284.6 eV. Before XPS studies, the ACs samples were degassed under vacuum at 100 °C for 24 hours to remove adsorbed pollutants. The microstructures of the ACs samples were studied using scanning electron microscopy (SEM; JEOL JSM-7800 F). At 196 °C, nitrogen adsorption/desorption isotherms were measured. The quenched solid density functional theory model was used to compute the specific surface area (SSA) and pore volume (PV), with the pore geometry assumed to be slit-shaped. The particle size distributions of the prepared carbons were measured using a Malvern Mastersizer 3000 laser diffraction particle size analyzer. The Aero-S dry powder dispersion device was used to disperse representative carbon samples.

A Solartron 1470E potentiostat was used to perform galvanostatic charge−discharge tests with varying applied current densities. Using the Galvanostatic charge−discharge method at 5 A g^{-1} for 3000 cycles, the cycle life stability of several AC electrodes was determined. The leakage current was measured after the cells were held at the set voltage for 2 h. A custom-made electrochemical cell with a pressure gauge with a 0.5 kPa precision was used to assess the gas evolution of the ACs electrodes. After 6 hours, the pressure increase in the symmetrical cell was measured using galvanostatic charging at various voltages. The impedance parameters were characterized using Electrochemical Impedance Spectroscopy (EIS) before and during cell aging. A BioLogic VSP-300 potentiostat was used to control the frequency range and voltage amplitude, which were set at 105−102 Hz and 10 mV, respectively.

3. Results and discussions

3.1 Physical and chemical properties

Gas sorption tests were used to examine the SSA of single carbon and composite carbon powders, as well as their pore properties. The QSDFT SSA and PV of the prepared carbon powders are listed in Table 1. The SSA of 0.25C4+0.75C8 carbon composite was greater than that of other carbon composites, with values of 1900, 2000, and 2102 m^2g^{-1} for 0.75C4+0.25C8, 0.50C4+0.50C8, and 0.25C4+0.75C8 carbon composites, respectively. C8 carbon powder exhibited a higher SSA (2110 m^2g^{-1}) than C4 and C12 carbon powders, which had 1809 and 1889 m^2g^{-1}, respectively, as active raw materials. The produced carbon powder's pore volume follows the same pattern as the SSA properties.

Laser diffraction was used to determine the particle size distribution of single carbon and composite carbon powders, and the results are expressed as volume basis. As listed in Table 1, The average particle size of C4, C8, and C12 carbon powders were 4.0, 8.2, and 11.9 µm, respectively. The average particle size of the carbon composite powder increases as the large particle size (C8) increases, resulting in 5.1, 5.9, and 6.2 µm for 0.75C4+0.25C8, 0.50C4+0.50C8, and 0.25C4+0.75C8, respectively. In general, as the average particle size increases, the volume percentage of smaller particles decreases, and the fraction of particles smaller than 1 µm reduces as well. The ash content of the prepared ACs powders was determined using a thermogravimetric analyzer after heating the samples in the air to 850 °C. All of the prepared ACs powders had a purity of less than 0.04 wt%, indicating good purity.

Table 1. The prepared carbons' SSA, particle size, and ash content

Physical properties	C4	0.75C4+0.25C8	0.50C4+0.50C8	0.25C4+0.75C8	C8	C12
Surface Area, m^2g^{-1}	1809	1900	2000	2102	2110	1889
Pore Volume, cm^3g^{-1}	0.933	0.990	1.005	1.013	1.021	0.957
D10, *(µm)*	1.1	1.8	2.5	2.2	3.7	4.5
D50, *(µm)*	4.0	5.1	5.9	6.2	8.2	11.9
D90, *(µm)*	10.5	12.4	14.5	13.3	18.5	22.1
<1µm, *(%)*	10.5	9.8	8.7	8.2	7.9	6.8
Ash, *(%)*	0.04	0.04	0.04	0.03	0.03	0.03

Table 2. Oxygen containing functional groups of the prepared carbons computed from XPS spectra

Surface Functional groups	C4	0.75C4+0.25C8	0.50C4+0.50C8	0.25C4+0.75C8	C8	C12
C, at.%	93.5	94.0	94.8	95.1	95.6	97.1
O, at.%	6.5	6.0	5.2	4.9	4.5	2.9
Phenol, % (C-OH)	19.7	18.6	17.2	16.9	14.2	10.4
Lactone, % (C-OOR)	4.2	4.1	3.9	3.8	3.7	2.9
Carboxylic, % (C-OOH)	4.5	3.8	3.0	2.7	1.9	1.9
Total, %	28.4	26.5	24.1	21.4	19.6	15.0

Table 2 shows the XPS spectra used to determine the concentration of surface functional groups on the produced ACs powders. The concentration of oxygen functional groups decreased with increasing average particle size, according to XPS analyses. The oxygen functional groups concentrations in 0.75C4+0.25C8, 0.50C4+0.50C8, and 0.25C4+0.75C8 carbon composites were 26.5, 24.1, and 21.4 %, respectively, suggesting that the big particle fractions had a substantial impact on the surface functional groups concentration. SEM was used to examine the morphology and structure of the C4, C8, C12, and all composites. The results are shown in Figure 1a−d, respectively. The manufactured ACs powder particles have a similar shape and surface morphology, but large and small particles have a varied quantity of fractions.

3.2 Electrochemical performances

The charge-discharge curves obtained at 0.5 Ag^{-1} for cells using each of the investigated carbons are shown in Figure 2a. The fact that they are all nearly triangle-shaped perfect capacitors implies that charge storage is controlled by the double-layer process.

At the lowest current density of 0.5 Ag^{-1}, 0.25C4+0.75C8 electrode generates the highest cell capacitance of 120 Fg^{-1} and it produces the highest cell capacitances of all samples at each of the current densities studied as listed in Table 3. Because the C8 electrode has a little bigger surface area

and pore volume than the former electrode, this could be an unexpected finding if only the specific surface area of the samples is considered, as listed in Table 1. This suggests that changes in behaviour are due to differences in particle size and distribution rather than the porosity.

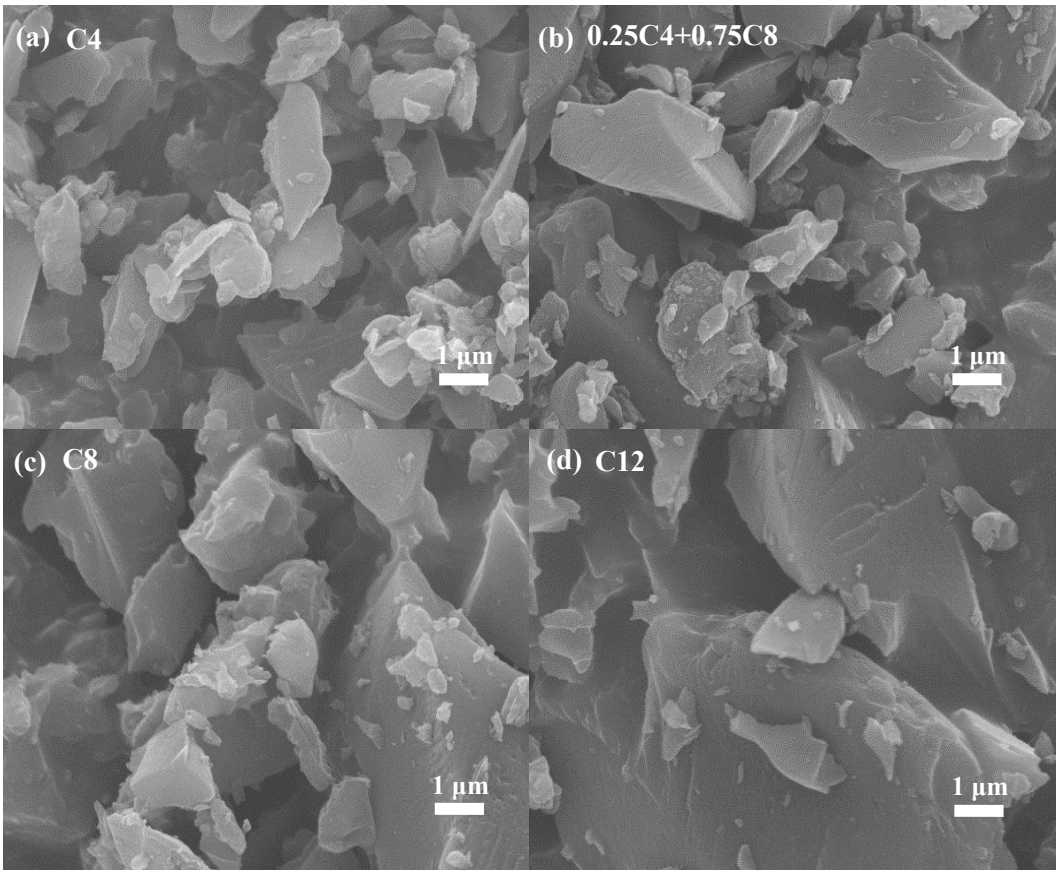

Figure 1. Morphology of the prepared carbons observed by SEM (a) C4, (b) 0.25C4+0.75C8, (c) C8, (d) C12

Except for C8 and C12, the specific capacitance of C4 carbon powder increases with an increasing number of large particles (C8) at a low rate of 5 Ag^{-1}. Among the prepared electrodes, 0.25C4+0.75C8 electrodes showed better high rate performance, probably due to their lower contact resistance (R_{inter}) and higher apparent diffusion coefficient (D_a), which is beneficial for ion transport. Previous research has shown that increasing the volume fraction of smaller particles increases cell resistance [6]. Increases in the fraction of fine particles and the breadth of the particle size distribution led to greater void values, according to other studies [10]. With increasing discharge rate, the C8 and C12 electrodes showed poor capacitance retention due to increased ion diffusion length in the big particle porosity. Figure 2b shows that the 0.25C4+0.75C8 electrode had the best cycling stability of all of the tested electrodes. Figure 2c shows that reducing the fractional size of smaller carbon particles (0.25C4+0.75C8) increased the energy density of cells in organic electrolytes. Due to its higher film density than the other electrodes, the carbon composite electrode also had a higher volumetric capacitance than the others.

As shown in Figure 2b and listed in Table 4, the interfacial contact resistance (R_{inter}) values of the C4, 0.75C4+0.25C8, 0.50C4+0.50C8, 0.25C4+0.75C8, C8, and C12 cells were 4.8, 4.1, 3.7, 3.0, 2.8, and 2.4 Ω respectively. The large particle ratio is consistent with this tendency. Lower interfacial resistance was associated with a larger percentage of the large particle (C8) or increased particle size.

The apparent diffusion coefficients (D_a) of Nyquist plots can be determined using the sloping line at the intermediate frequency. As summarized in Table 4, this is due to the retention of surface area and pore structure, as well as the comparatively low percentage of smaller particles (C4), which improved film density, reduced interfacial contact resistance (R_{inter}), and hence facilitated electrolyte ion movement within ACs pores.

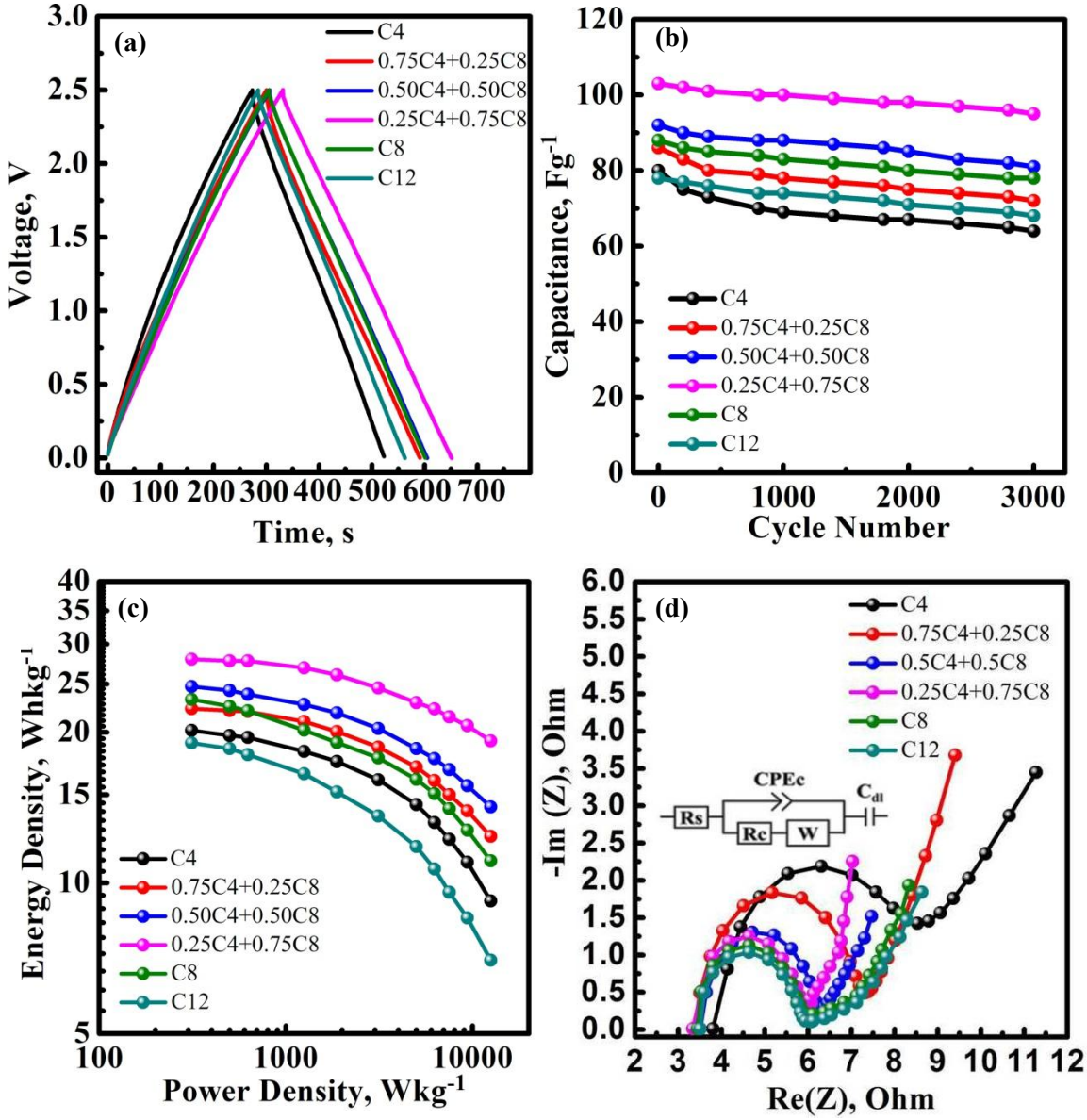

Figure 2. Electrochemical performance of various carbon electrode; (a) charge−discharge curve at 0.5 A g^{-1}, (b) Ragone Plots, (c) Cycle stability at 5 A g^{-1}, and (d)cell' EIS spectrum.

Table 3. Physical characteristics, specific capacitance (gravimetric and volumetric), high rate retention, and cycle life stability of the prepared carbons

	C4	0.75C4+0.25C8	0.50C4+0.50C8	0.25C4+0.75C8	C8	C12
Coating Thickness, *μm*	30	30	30	30	30	30
Carbon Weight, *mg*	0.89	1.20	1.75	2.57	2.64	2.68
Film density, *g cm^{-3}*	0.22	0.30	0.44	0.65	0.66	0.67
Tap density, *g cm^{-3}*	0.29	0.29	0.29	0.31	0.33	0.36
Gravimetric Cap. at 0.5 Ag^{-1}, *(F g^{-1})*	101	108	115	120	110	99
Volumetric Cap. at 0.5 Ag^{-1}, *(F cm^{-3})*	24	33	51	78	73	66
Gravimetric Cap. at 20 Ag^{-1}, *(F g^{-1})*	63	69	75	83	66	58
High Rate Ret. ($C_{20}/C_{0.5}$), *(%)*	62	64	65	69	60	59
Cycle life Ret. (C_{3000}/C_1), *(%)*	80.1	84	88	92	89	87

Table 4. Bulk Electrolyte Resistance (R_s), Interfacial Contact Resistance (R_{inter}), and Apparent Diffusion Coefficient (D_a) for diverse samples are quantified using EIS spectra.

	C4	0.75C4+0.25C8	0.50C4+0.50C8	0.25C4+0.75C8	C8	C12
R_s, *Ω*	1.5	1.4	1.3	1.3	1.4	1.4
R_{inter}, *Ω*	4.8	4.1	3.7	3.0	2.8	2.4
D_a, *cm^2 s^{-1}*	4.1×10^{-7}	4.5×10^{-7}	4.9×10^{-7}	6.56×10^{-7}	3.56×10^{-7}	2.86×10^{-7}

3.3 Electrode reliability

After holding the cells at a steady voltage for 2 hours, the leakage current was measured. There should be no leakage current during the open circuit for perfect capacitors. As shown in Figure 3a, the leakage current of the smaller carbon particle electrodes (C4) increased considerably after 2.6 V. It was significantly higher than that of the carbon composite electrode (0.25C4+0.75C8) and the large carbon particle electrodes (C8 and C12), owing to the significant decomposition of oxygen-containing functional groups [15,16] and the electrolyte decomposition resulting from interactions with the

smaller particles [6]. The leakage current was measured to be on the order of C4 > C12 > C8 > 0.25C4+0.75C8.

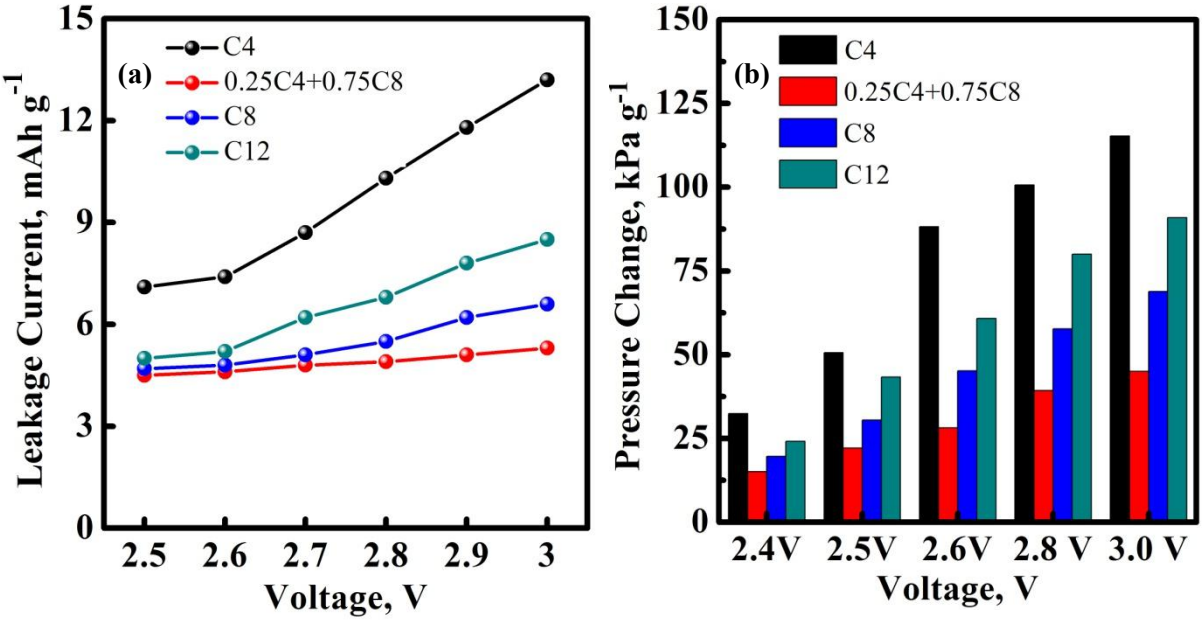

Figure 3. (a) Charge Leakage, (b) Inside gas pressure of the produced cells measured at different voltages.

The gas pressure of the prepared cells, which were maintained at a given voltage for 6 hours, is shown in Figure 3b. The produced gas has the potential to degrade capacitor performance and potentially cause mechanical damage such as rupture, cell leakage, and lower electrode performance and reliability. As shown, the C4 cell exhibits the highest cell pressure at the range of applied voltage. However, the cells containing the big carbon particle showed less gassing. 0.25C4+0.75C8 cells have the lowest cell pressure among the large particle-contained carbon electrodes. The gas evolution tendency, regardless of voltage, is C4 > C12 > C8 > 0.25C4+0.75C8, which is consistent with the leakage current. These findings support the hypothesis that a carbon composite with a high proportion of big carbon particles effectively suppresses undesirable faradic side reactions. According to a previous study, reducing average particle size and increasing the fraction of small particles exposes more graphitic edges and produces highly reactive carbon-carbon bonds. When exposed to ambient oxygen, these sites react, forming surface functions that can participate inside reactions with electrolytes [17, 18].

4. Conclusions

Finally, in terms of electrochemical performance and reliability, carbon composite electrodes outperform single carbon electrodes. Carbon composite with 0.25C4+0.75C8 composition provides a higher capacitance value, high retention rate, extended cycle life, and good reliability. Large carbon particles can reduce electrical resistance, increase ionic diffusion, and decrease undesired faradic reactions at the interface between the carbon and electrolyte surfaces when used in the right proportion. The carbon electrode composite made up of small and large particles can increase the electrode's film density and specific capacitance, consequently boosting the volumetric capacitance needed for industrial applications.

Acknowledgments
The financial support provided for this work by the Ministry of Science and Technology (MOST) of Taiwan, and The Indonesia Ministry of Education and Culture are gratefully appreciated.

References

[1] Deng, Y. Review on recent advances in nitrogen-doped carbons: preparations and applications in supercapacitors, J. Mater. Chem A, vol. 4, p. 1144–1173, 2016
[2] N. Kularatna. Benefits of Million Times Larger Capacitance in EDLCs: Supercapacitor Assisted Novel Circuit Topologies, APIC 2017, Wellington, New Zeland, 2017
[3] R. Pietrzak, K. Jurewicz, P. Nowicki, K. Babel, and H. Wachowska. Microporous activated carbons from ammoxidised anthracite and their capacitance behaviours, Fuel, 86, 1086, 2007
[4] J. Chmiola, G. Yushin, Y. Gogotsi, C. Portet, P. Simon, and P. L. Taberna. Anomalous Increase in Carbon Capacitance at Pore Sizes Less Than 1 Nanometer, Science, 313, 1760, 2006
[5] E. Frackowiak and F. Beguin. Electrochemical storage of energy in carbon nanotubes and nanostructured carbons, Carbon, 40, 1775, 2002
[6] Anthony J. R. Rennie, Vitor L. Martins, Rachel M. Smith, Peter J. Hall. Influence of Particle Size Distribution on the Performance of Ionic Liquid-based Electrochemical Double Layer Capacitors. Scientific Reports, 6, 22062, 2016.
[7] Yoshida, A., Nonaka, S., Aoki, I., Nishino, A. Electric double-layer capacitors with sheet-type polarizable electrodes and application of the capacitors. J. Power Sources 60, 213−218, 1996.
[8] Portet, C., Yushin, G., Gogotsi, Y. Effect of Carbon Particle Size on Electrochemical Performance of EDLC. J. Electrochem. Soc. 155, A531−A536, 2008.
[9] Pandolfo, A. G., Wilson, G. J., Huynh, T. D., Hollenkamp, A. F. The influence of conductive additives and inter-particle voids in carbon EDLC electrodes. Fuel Cells 10, 856−864, 2010.
[10] Yu, A. B., Bridgwater, J., Burbidge, A. On the modelling of the packing of fine particles. Powder Technol. 92, 185−194, 1997.
[11] Yang, R. Y., Zou, R. P., Yu, a. B. Computer simulation of the packing of fine particles. Phys. Rev. E-Stat. Physics, Plasmas, Fluids Relat. Interdiscip. Top. 62, 3900−3908, 2000.
[12] McGeary, R. K. Mechanical Packing of Spherical Particles. J. Am. Ceram. Soc. 44, 513−522, 1961.
[13] Nolan, G. T., Kavanagh, P. E. Computer simulation of random packing of hard spheres. Powder Technol. 72, 149−155, 1992.
[14] Rouault, Y., Assouline, S. A probabilistic approach towards modeling the relationships between particle and pore size distributions: the multicomponent packed sphere case. Powder Technol. 96, 33−41, 1998.
[15] Yoshida, A.; Tanahashi, I.; Nishino, A. Effect of Concentration of Surface Acidic Functional Groups on Electric Double Layer Properties of Activated Carbon Fibers. Carbon 1990, 28, 611−615
[16] Nguyen, Q. D.; Wu, Y. H.; Wu, T. Y.; Deng, M. J.; Yang, C. H.; Chang, J. K. Gravimetric/Volumetric Capacitances, Leakage Current, and Gas Evolution of Activated Carbon Supercapacitors. Electrochim.Acta 2016, 222, 1153−1159
[17] Harker, H., Horsley, J. B., Robson, D. Active centres produced in graphite by powdering. Carbon N. Y. 9, 1–9 (1971).
[18] Beguin, F., Frackowiak, E. Carbons for Electrochemical Energy Storage and Conversion Systems. (CRC Press, 2010).